A Modeling Assessment of Using Optical Fiber Devices For Electric Field Measurements

David Alumbaugh[1], Evan Um[1], Michael T. V. Wylie[2] and Bjorn Paulsson[2]
[1]Lawrence Berkeley National Laboratory, One Cyclotron Road, Berkeley, CA 94720
[2]Paulsson, Inc, 16543 Arminta Street, Van Nuys, CA 91406-1745

SUMMARY

In this paper, we describe numerical studies that have been undertaken to investigate the plausibility of using fiber-optic sensing technologies for the measurement of electric fields in geophysical applications. An initial study simulating a single fiber wrapped with a piezoelectric polymer (polyvinylidene fluoride or PVDF) showed too low a sensitivity for geophysical applications except in very specialized down-hole monitoring situations. This led to a second study whereby we simulated fiber being wound around cores composed of lead zirconate titanate (PZT), a ceramic with high piezoelectric properties, using two different 'polling' and winding configurations. After a brief introduction to the possible advantages of measuring electric fields using fiber optics, we will discuss the numerical modeling results and present conclusions on the way forward with this measurement technology.

Keywords: electric field, piezoelectric, fiber optic sensing

INTRODUCTION

In the last 10 years we've seen a rapid increase in the deployment of fiber optic sensors for geophysical sensing. As described in Hartog (2017), measuring small changes in travel-time in pulses of laser light within glass fibers due to the stretching or contraction in the fiber allows for novel deployments in well completions and surface installations of Distributed Acoustic Sensing (DAS), Distributed Strain Sensing (DSS), and Distributed Temperature Sensing (DTS) measurements. In addition to the relatively inexpensive sensor installation and the fact that the fiber provides nearly continuous – high spatial resolution measurements along its length, a principal attraction of these type of measurements for permanent installations is that there are no buried or downhole electronics. That is, only the fiber is subsurface and all the electronics are contained in the interrogator which is housed on the surface and can be easily accessed. This provides an advantage over traditional permanent subsurface installations where electronics are buried and often serve as a point of failure.

Due to the advantages of not having downhole electronics, Alumbaugh et al. (2022) numerically investigated the plausibility of a downhole completion that would enable electric field measurements along either the outside or inside of a well completion. As shown in Figure 1, the model assumed a fiber wrapped with polyvinylidene fluoride (PVDF), which is a flexible polymer that has relatively high piezoelectric constants (d_{33} and d_{13}) that transduce electrical to mechanical energy (and vice-versa) for a non-ceramic material. Note that 'poling' the material such that the produced mechanical strain is in the same direction as the electric field of interest is given by the d_{33} value, while poling the material to produce a d_{13} value indicates a strain will be produced perpendicular to the electric field of interest.

Though PVDF has piezoelectric constants that are smaller than those of high-piezoelectric ceramics such as lead zirconate titanate (PZT), the polymer was chosen as the material due to its flexibility as it was assumed that ceramic materials would fracture and break during common fiber installation practices for subsurface well completions. Thus, the work of Alumbaugh et al. (2022) assumed that the PVDF was poled to produce d_{13} values between 4 and 23 ($x10^{-12}$ m/V) which would cause the fiber to stretch along a well casing due to electric fields perpendicular to the casing. The numerical study indicated that this type of fiber measurement was far too insensitive to most electric field measurements of geophysical interest (i.e. the noise level was estimated to be 10's of mV/m). However, it was noted that if an electric source could be placed downhole, optical measurements in the vicinity of the source could be used to define the oil/water mixture as well as identify water wet versus oil wet fracture zones post fracking operations.

Though the initial study strongly suggested that a single fiber with a piezoelectric coating would not provide the electric field sensitivity required for most geophysical applications, it did suggest that layers of fiber wound around a PZT may produce high enough sensitivity to warrant long-term deployment in downhole or sea floor environments to provide monitoring of carbon-sequestration operations. Therefore, LBNL recently

partnered with Paulsson, Inc., a small company with experience in building high sensitivity fiber-based acoustic and acceleration sensors, to submit a successful Phase 1 proposal to the US Department of Energy's (DOE's) Small-Business Innovative Research (SBIR) program (DE-SC0023609). In the remainder of this paper we first describe the sensor configurations that were simulated using a modified version of the SIMPEG2D code described in Heagy and Oldenburg (2019), and then describe the workflow used to convert calculated electric fields to mechanical strain in the fiber which allows us to estimate the electric field noise floor per layer of fiber wound around piezoelectric cores. Ultimately these theoretical noise floor estimates will be compared to lab measurements of sensors that are currently being assembled in Paulsson, Inc.'s Van Nuys, CA facilities.

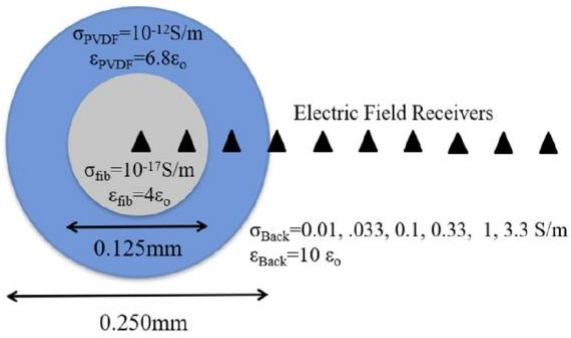

Figure 1: Electromagnetic properties of the model used to simulate the electromagnetic response of a PVDF-coated glass fiber in an otherwise homogeneous medium as simulated by Alumbaugh et al. (2022).

ELECTROMAGNETIC MODELS AND SIMULATIONS

For the lab measurements that will be undertaken in Phase 1 of this SBIR project, we are working with APC International, Ltd (https://www.americanpiezo.com/) to manufacture and supply the piezoelectric materials necessary to build the transducer. To build the electromagnetic property models as well as estimate the strain the cores will place on the fiber, we used electromagnetic material and piezoelectric values for two different PZT materials from a book published by the company (APC International Ltd.,2011) which are given in Table 1. Note that the PZ840 and PZ855 represent end members of the PZT offerings from APC in terms of the loss tangent values that were used to determine the conductivities and dielectric constants, as well as the piezoelectric constants. In addition to providing a theoretical analysis for these two different materials, we also tested two different core and winding configurations as shown in Figure 2; a core that uses end-to-end windings to make use of d_{33}-generated strain produced along the length of the core in the same direction as that of the electric field being measured, as well as a 'solenoidal' type of winding that makes use of d_{31}-generated strain in the direction radially perpendicular to that of the electric field being 'measured'. Note that the core for the latter is a hollow cylinder which is necessary to property 'pole' the material with a d_{31} piezoelectric constant and the fiber for the former will be wound around caps on the top and bottom such that the minimum bending radius of the fiber is maintained.

Material	σ(S/m)	ε(F/m)	d_{33}(m/V)x10^{-12}	d_{31}(m/V)x10^{-12}
PZ840	$2.7x10^{-7}$	$1.1x10^{-8}$	$2.9x10^{2}$	$1.25x10^{2}$
PZ855	$6.1x10^{-6}$	$3.6x10^{-8}$	$6.3x10^{2}$	$2.76x10^{2}$

Table 1: Electromagnetic and piezoelectric properties of two different lead-zirconate compounds examined in this study. From APC International Ltd. (2011).

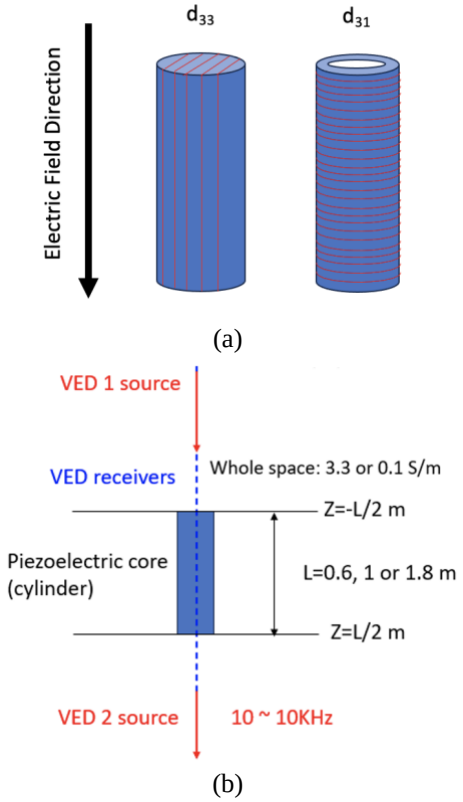

Figure 2: (a) Two different core and optical winding configurations simulated in this study. The red lines represent the optical fiber winding directions for the two cases, while the blue solids represent the shape of the piezoelectric core material. In the left most wind the transducer will have caps that ensure the minimum bending radius of the fiber is maintained. (b) A vertical cross-section through the solid cylinder model showing how the model was set up. Note that the diameter of the core is 5cm.

The numerical algorithm used is a version of SIMPEG2D (Heagy and Oldenburg, 2019) that has been modified to account for the dielectric constant values shown in Table 1 via the inclusion of a complex conductivity term. A

vertical cross section through the solid cylinder model with dimensions and resistivity values outside of the core are shown in Figure 2b. In order to produce a fairly uniform vertical electric field across the region of interest, two electric dipoles were used with one located 4m off each end of the core as shown in Figure 2b. Calculations of the electric fields were made at different locations within the core as well as just outside of it at 10Hz, 100Hz, 1kHz, and 10kHz. Note that for geophysical applications we want to go to lower frequencies; however, the numerical solution became less stable below 10Hz. Thus, for initial testing, we limited the calculations to 10-10,000 Hz. In terms of background resistivities we used two; 0.1S/m and 3.3S/m to represent 'average' earth and sea-water conductivity values.

Examples of the electric field calculations for the solid PZ855 core embedded in sea-water are shown in Figure 3 with 3a depicting the 100 Hz results and 3b depicting the 10 kHz solution. Here E_Z represents the 'vertical' electric field we are trying to measure with the piezoelectric device, and E_X the radial or horizontal component. Note that; 1) the electric field amplitudes are 'amplified' across the core boundary due to the much higher resistivity of the core material compared to that of the background; 2) the vertical electric field is fairly uniform in amplitude along the length of the core as well as with radial position; 3) the vertical electric fields are at least one order of magnitude higher than the strongest horizontal fields; and 4) the horizontal field amplitude goes to zero at the center of the core which is caused by the orientation of the two electric dipoles. Because we are only interested in 'measuring' the vertical field, which is much stronger than the horizontal, we don't need to worry about the behavior of the horizontal field.

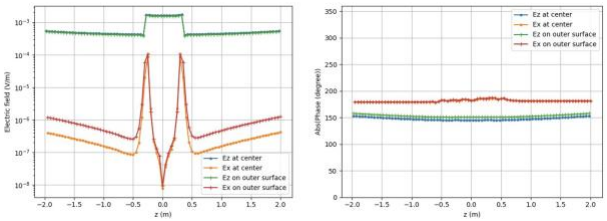

(a)

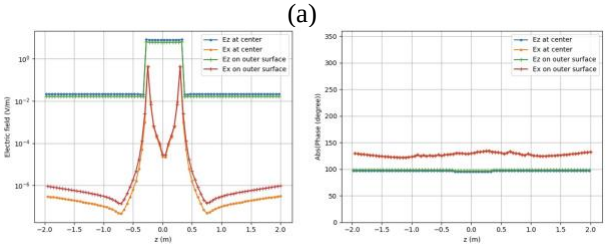

(b)

Figure 3: Electric field calculations for the solid PZ855 core located in seawater at (a) 100 Hz and (b) 10 kHz. Here E_Z represents the electric field which we are interested in measuring and E_X the horizontal or radial field. The two sets of calculations are for the center of the model and for just inside the edge of the core. The left-hand figure is amplitude and the right-hand is phase. Note that the phase calculations are not used in the subsequent piezoelectric transducer noise calculations.

PIEZOELECTRIC SENSOR NOISE-FLOOR ESTIMATES

To estimate electric field noise floor estimates we used the following workflow for the two optical fiber winding configurations.

1. Calculate number of turns of fiber per core for 105μm diameter fiber (up-buffered polyimide coating):
   a. Hollow cylinder with solenoidal windings: 5442 turns.
   b. Solid cylinder assuming 2cm square plates with end-to-end windings: 459 turns.
2. Calculate length of stretchable fiber for a single winding layer of core assuming number of turns given above:
   a. Hollow cylinder with solenoidal windings: 391m.
   b. Solid cylinder with end-to-end windings: 466m.
3. Use the calculated vertical electric fields from the modeling described in the previous section:
   a. Inside core:
      i. Hollow cylinder: just inside outer edge.
      ii. Solid cylinder: in center of core.
   b. Outside core.
4. Multiply Piezoelectric Charge Constant in Table 1 by electric field inside core to determine the piezoelectrically generated strain produced on the fiber.
5. Multiply calculated strain by stretchable length of fiber determined in 2) to get amount of fiber-stretch per layer of optical fiber windings.
6. Divide the amount of fiber stretch by the interrogator noise floor (7.4E-11m) and multiply the electric field outside of the core in the homogenous medium by this ratio. This provides the estimated electric field noise floor or conversely, the sensitivity of the sensor.

The optical noise floor is derived from commercial optical sensing systems utilizing interferometric sensing configurations. The estimated noise floor as a function of frequency that are estimated by applying this workflow for the two different core and winding geometries in Figure 1 are given in Figure 4a for the solenoidal winding geometry and Figure 4b for the end-to-end winding configuration. The four curves in each plot represent results for different core materials and background resistivities. Note that the core material has a much bigger effect on the noise floor than the background resistivity. The higher sensitivity/lower noise floor provided by the PZ840 material is likely due to it having over an order of magnitude lower resistivity than PZ855, even though the PZ840m also has a lower piezoelectric charge constant. Also note that the end-to-end winding produces better noise-floors than the solenoidal winding for the same size

core. This can be expected due to the larger d_{33} values shown in Table 1 when compared to d_{31}. Lastly, note that the noise floor increases (i.e. sensitivity decreases) as the frequency gets lower. This most likely is due to the ratio of E_Z inside the core to outside the core decreasing with decreasing frequency as shown when comparing Figure 3a to 3b.

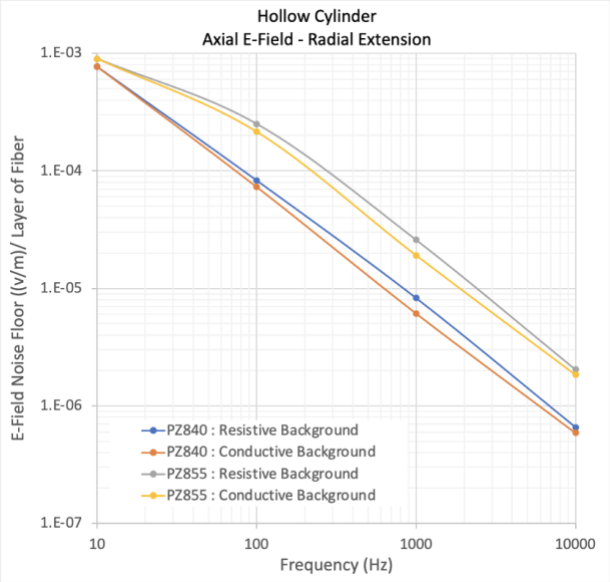

(a)

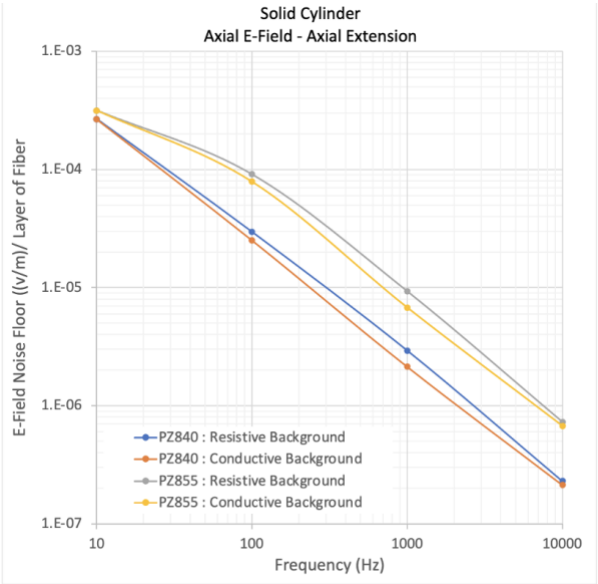

(b)

Figure 4: Electric field noise floors as a function of frequency estimated for the a) solenoidal-hollow cylinder core configuration shown in Figure 1, and the (b) solid core – end-to-end winding sensor configuration. The blue and red curves represent estimates for the PZ840 material embedded in the two different background resistivities, and the yellow and grey curves for the PZ855 PZT.

DISCUSSION

The numerical results for optical fiber sensing of electric fields that we have presented makes assumptions that may result in inaccurate predictions. Most notable of these is that the conductivities and dielectric permitivities given in Table 1 that were used in the modeling effort were derived from the book provided by the manufacturer (APC International Ltd.,2011). Independent internet searches have shown reported conductivities of PZT to be much lower; however, modeling of these lower conductivity materials imply a high contrast between the background and core material which can result in numerical instabilities. A second factor that we have not included here is the possibility that other electric field components (i.e. E_X and E_Y) could also cause a response in the piezoelectric material which could contaminate the response. On the other hand, the noise floor calculations assume a single layer of fiber on 0.6 m long cores. More wraps of fiber as well as longer cores will only improve the sensitivity. In any event, the next step in this project is to build prototypes of the sensors simulated in this paper and measure the frequency response in a small water filled tank. This will allow us not only to determine the accuracy of our calculations, but also determine if further studies of this type of sensor is warranted.

CONCLUSION

In this paper we have presented a numerical study to examine the possibility of making electric field measurements using optical fiber wound around different PZT materials. Though the results look promising, the estimated electric field sensitivities (~0.1mV at 10Hz to 0.1 μV/m at 10kHz) still look less than the 1pV/m to 1nV/m noise floors provide by connecting two electrodes up in a dipole configuration. Thus, the next phase of this project will involve making measurements on prototype sensors in the lab. After these measurements are made we will look at methods to enhance the sensitivity to determine if this type of electric field sensor is worth pursuing.

ACKNOWLEDGMENTS

Work for this project has been funded via the DOE's Small Business Innovative Research (SBIUR) program under grant DE-SC0023609. The authors would also like to thank Professor Lindsey Heagy from the University of British Columbia and the rest of the SIMPEG group for providing the modifications to the SIMPEG2D code that were necessary to make these calculations.

REFERENCES

Alumbaugh, D. L., Um, E. S., Hoversten, G. M., and Key, K., 2021, Distributed electric field sensing using fibre optics in borehole environments; Geophysical Prospecting, **70**(1), 210-221.

APC International, LTD, 2011, Piezoelectric Ceramics: Principles and Applications, APC International.

Hartog, A. H., 2017, An Introduction to Distributed Optical Fibre Sensors; CRC Press, https://doi.org/10.201/9781315119014.

Heagy, L.J. and Oldenburg, D.W., 2019. Modeling electromagnetics on cylindrical meshes with applications to steel-cased wells. *Computers & Geosciences*, *125*, pp.115-130.